JOC Article

Tetrathiafulvalene in a Perylene-3,4:9,10-bis(dicarboximide)-Based Dyad: A New Reversible Fluorescence-Redox Dependent Molecular System

Stéphanie Leroy-Lhez,* Jérôme Baffreau, Lara Perrin, Eric Levillain,* Magali Allain, Maria-Jesus Blesa,† and Piétrick Hudhomme*

Chimie, Ingénierie Moléculaire et Matériaux d'Angers, UMR CNRS 6200 - Université d'Angers, 2 Bd Lavoisier, 49045 Angers, France

pietrick.hudhomme@univ-angers.fr

Received April 15, 2005

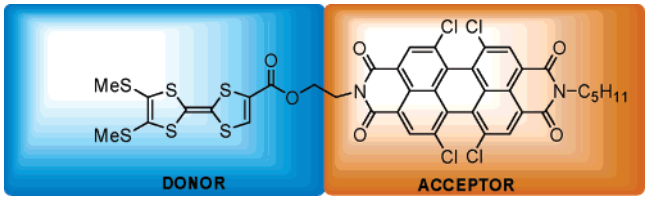

A donor−acceptor dyad system involving tetrathiafulvalene (TTF) as donor attached by a flexible spacer to perylene-3,4:9,10-bis(dicarboximide) (PDI) as acceptor was synthesized and characterized. The strategy used the preliminary synthesis of an unsymmetrical PDI unit bearing an alcohol functionality as anchor group. Single-crystal analysis revealed a highly organized arrangement in which all PDI molecules are packed in a noncentrosymmetrical pattern. It was shown that the fluorescence emission intensity of the TTF−PDI dyad can be reversibly tuned depending on the oxidation states of the TTF unit. This behavior is attributed to peculiar properties of TTF linked to a PDI acceptor, which fluoresces intrinsically. Consequently, this dyad can be considered as a new reversible fluorescence-redox dependent molecular system.

Introduction

Tetrathiafulvalene (TTF) **1**, first synthesized in the early 1970s,[1] is still among the most studied heterocyclic system. Discovery of TTF-based organic conductors[2] has initiated the development of major research activities in the search for novel applications in materials science.[3] Progress in the synthesis of more and more sophisticated TTF-based architectures and the wide diversity of corresponding electronic materials was very recently reviewed.[4] In particular, donor−acceptor (D−A) molecular systems built around this strong π-donor TTF have been the focus of intensive investigations in recent years.[5] Objectives concern the fine-tuning of the HOMO−LUMO gap for these molecules with the aim of realizing unimolecular electronic devices and the investigation of charge, energy, or electron-transfer processes involved between TTF and acceptor counterparts. Thus, TTF derivatives proved to be excellent building blocks for intramolecular charge transfer (ICT) interaction[6] and the photoinduced electron-transfer process,[7] especially involving C_{60} as the acceptor.[8] These topics are of general interest especially because of their importance in molecular electronics,[9] artificial mimicking of photosynthesis, and solar energy conversion.[10] It was also demonstrated that TTF can act as a suitable bridge to promote intramolecular electron transfer between two redox centers.[11] One of the most interesting properties of TTF

† Permanent address: Departamento Quimica Organica, Facultad Ciencias, Universidad de Zaragoza, C. Pedro Cerbuna 12, 50009 Zaragoza, Spain.

(1) Wudl, F.; Smith, G. M.; Hufnagel, E. J. *J. Chem. Soc., Chem. Commun*. **1970**, 1453.

(2) Ferraris, J.; Cowan, D. O.; Walatka, V. V.; Perlstein, J. H. *J. Am. Chem. Soc.* **1973**, *95*, 948.

(3) (a) Bryce, M. R. *J. Mater. Chem.* **2000**, *10*, 589. (b) Segura, J. L.; Martín, N. *Angew. Chem., Int. Ed.* **2001**, *40*, 1372.

(4) (a) Special issue on Molecular Conductors: *Chem. Rev*. **2004**, *104*, 4887; Batail, P., Ed. (b) *TTF chemistry: Fundamentals and applications of tetrathiafulvalene*; Yamada, J.-i., Sugimoto, T., Eds.; Springer-Verlag: Berlin, 2004.

(5) Bendikov, M.; Wudl, F.; Perepichka, D. F. *Chem. Rev*. **2004**, *104*, 4891.

(6) Bryce, M. R. *Adv. Mater*. **1999**, *11*, 11.

(7) (a) *Photoinduced Electron Transfer*; Fox, M. A., Chanon, M., Eds.; Elsevier: Amsterdam, 1988. (b) Kurreck, H.; Huber M. *Angew. Chem., Int. Ed. Engl*. **1995**, *34*, 849.

(8) Martín, N.; Sánchez, L.; Illescas, B.; Pérez, I. *Chem. Rev*. **1998**, *98*, 2527.

(9) For a general review on molecular electronics, see: Carroll, R. L.; Gorman, C. B. *Angew. Chem., Int. Ed.* **2002**, *41*, 4378.

10.1021/jo050766n CCC: $30.25
Published on Web 07/01/2005

SCHEME 1

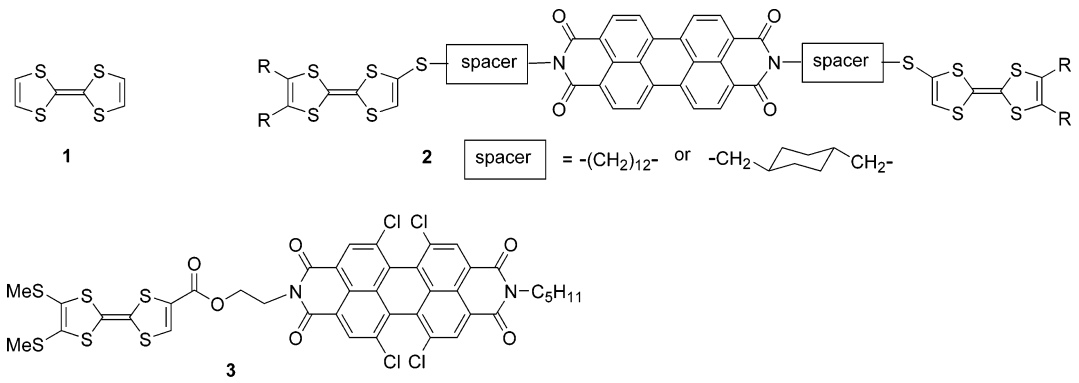

is that it can be oxidized successively and reversibly to the cation radical and dication species within a very accessible potential window. Consequently, the possibility of exploiting these multistage redox states (TTF^0, $TTF^{\bullet+}$, TTF^{2+}) was investigated to construct supramolecular systems[12] that can be controlled by external stimuli.[13] These unique electronic properties of TTF were also opportunely used with the elaboration of molecular systems such as TTF-based fluorescence-redox switches[14] when linked to different acceptors such as phthalocyanine,[15] porphyrin,[16] or anthracene.[17] But surprisingly, in the construction of TTF-based dyads, no example implies the highly fluorescent acceptor perylene-3,4:9,10-bis(dicarboximide) (PDI), certainly because of difficulties to manipulate such insoluble materials. Concerning this PDI accepting part, the possibility of developing light intensity-dependent molecular electronic switches has been demonstrated in a porphyrin−PDI−porphyrin triad.[18] To our knowledge, only triad architectures **2** involving one PDI unit and two TTF units have been recently reported and partial quenching of fluorescence was ascribed to a photoinduced electron-transfer process (Scheme 1).[19]

Consequently, we have been interested in assembling these two electroactive units with the synthesis of dyad **3** consisting of the acceptor PDI, which fluoresces intrinsically attached to the nonfluorescent TTF. Results obtained from a dyad system, with the 1/1 stoichiometry between donor and acceptor are expected to be unambiguous compared to those from a triad in which the role of the partner in excess is usually not really defined.

In this work, we report the synthesis and electrochemical and spectroscopic properties of dyad **3** and its oxidized species. This molecular system could finally act as a potential new fluorescence-redox dependent molecular system whose fluorescence emission intensity reversibly depends on the oxidation state of TTF.

Results and Discussion

Synthesis. The strategy to prepare dyad **3** was to use an esterification reaction between TTF monocarboxylic acid **4** and unsymmetrical PDI monoalcool **5** as key materials (Scheme 2). First, the synthesis of TTF monoacid **4** started by the trimethyl phosphite-induced cross-coupling reaction[20] of the 2-(thi)oxo-1,3-dithiole moieties giving 2,3-bis(methyloxycarbonyl)TTF derivative **6** in 59% yield.[21] Further monodecarboxymethoxylation was cleanly achieved using LiBr in refluxing DMF (95% yield), and subsequent ester hydrolysis of compound **7** afforded TTF monoacid **4** in 90% yield according to reported procedures.[22] This two-step transformation of the readily available diester **6** into the monocarboxylic acid **4** proved to give slightly better yields using LiBr in DMF than LiBr in HMPA.[23]

Second, unsymmetrical PDI **5**, tetrasubstituted by chlorine atoms at the bay region, was efficiently obtained by direct condensation of 1-pentylamine and 2-ethanolamine in stoichiometric ratio on 1,6,7,12-tetrachloroperylene tetracarboxylic dianhydride **9**. After precipitation of symmetrical PDI dialcool **11**, both symmetrical and unsymmetrical compounds **10** and **5**, respectively, were easily separated by silica gel column chromatography (Scheme 3).[24] Compound **10** will be used as reference compound for dyad **3** studies as compound **5** is not suitable by lack of solubility. Esterification between TTF

(10) (a) *Photoinduced Electron Transfer*; Fox, M. A., Chanon, M., Eds.; Elsevier: Amsterdam, 1988. (b) *Molecular Electronics Science and Technology*; Aviram, A., Ed.; American Institute of Physics: New York, 1992. (c) Gust, D.; Moore, T. A.; Moore, A. L. *Acc. Chem. Res.* **2001**, *34*, 40.

(11) (a) Gautier, N.; Dumur, F.; Lloveras, V.; Vidal-Gancedo, J.; Veciana, J.; Rovira, C.; Hudhomme, P. *Angew. Chem., Int. Ed.* **2003**, *42*, 2765. (b) Dumur, F.; Gautier, N.; Gallego-Planas, N.; Şahin, Y.; Levillain, E.; Mercier, N.; Hudhomme, P.; Masino, M.; Girlando, A.; Lloveras, V.; Vidal-Gancedo, J.; Veciana, J.; Rovira, C. *J. Org. Chem.* **2004**, *69*, 2164.

(12) The use of TTF as a building block in supramolecular chemistry was excellently reviewed: Nielsen, M. B.; Lomholt, C.; Becher, J. *Chem. Soc. Rev.* **2000**, *29*, 153.

(13) Balzani, V.; Credi, A.; Mattersteig, G.; Matthews, O. A.; Raymo, F. M.; Stoddart, J. F.; Venturi, M.; White, A. J. P.; Williams, D. J. *J. Org. Chem.* **2000**, *65*, 1924 and references therein.

(14) A fluorescence-redox switch is obtained if an oxidation/reduction of a switch molecule is combined with a photon read-out process.

(15) (a) Wang, C.; Bryce, M. R.; Batsanov, A. S.; Stanley, C. F.; Beeby, A.; Howard, J. A. K. *J. Chem. Soc., Perkin Trans. 2* **1997**, 1671. (b) Farren, C.; Christensen, C. A.; Fitzgerald, S.; Bryce, M. R.; Beeby, A. *J. Org. Chem.* **2002**, *67*, 9130.

(16) Li, H.; Jeppesen, J. O.; Levillain, E.; Becher, J. *Chem. Commun.* **2003**, 846.

(17) Zhang, G.; Zhang, D.; Guo, X.; Zhu, D. *Org. Lett.* **2004**, *6*, 1209.

(18) O'Neil, M. P.; Niemczyk, M. P.; Svec, W. A.; Gosztola, D.; Gaines, G. L.; Wasielewski, M. R. *Science* **1992**, *257*, 63.

(19) Guo, X.; Zhang, D.; Zhang, H.; Fan, Q.; Xu, W.; Ai, X.; Fan, L.; Zhu, D. *Tetrahedron* **2003**, *59*, 4843. The same result was observed for analogous triad containing TTF and naphthalene bis(dicarboximide) units: Guo, X.; Zhang, D.; Xu, W.; Zhu, D. *Synth. Met.* **2003**, *137*, 981.

(20) For reviews on TTF chemistry, see: (a) Garín, J. *Adv. Heterocycl. Chem.* **1995**, *62*, 249. (b) Schukat, G.; Fanghänel, E. *Sulfur Rep.* **2003**, *24*, 1.

(21) Blanchard, P.; Sallé, M.; Duguay, G.; Jubault, M.; Gorgues, A. *Tetrahedron Lett.* **1992**, *33*, 2685.

(22) Parg, R. P.; Kilburn, J. D.; Petty, M. C.; Pearson, C.; Ryan, T. G. *J. Mater. Chem.* **1995**, *5*, 1609.

(23) Devic, T.; Avarvari, N.; Batail, P. *Chem.−Eur. J.* **2004**, *10*, 3697.

SCHEME 2. Synthesis of Dyad TTF−PDI 3

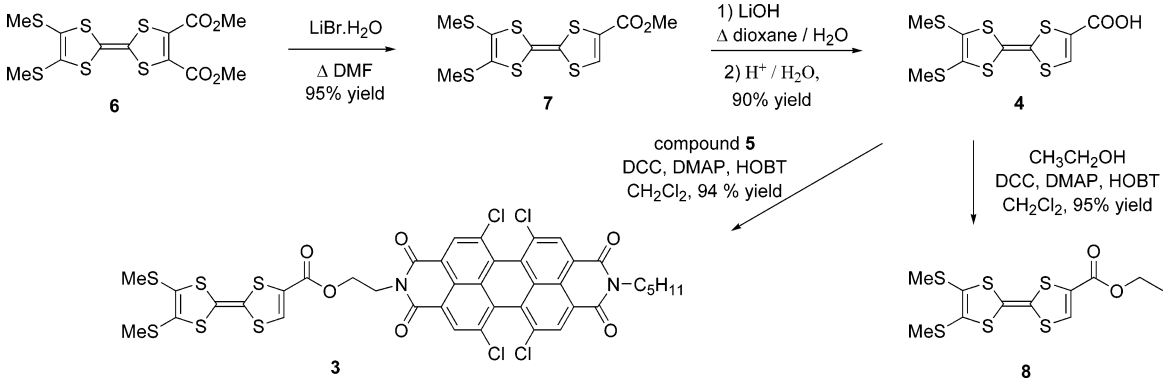

SCHEME 3. Strategy for the Synthesis of Unsymmetrical PDI 5

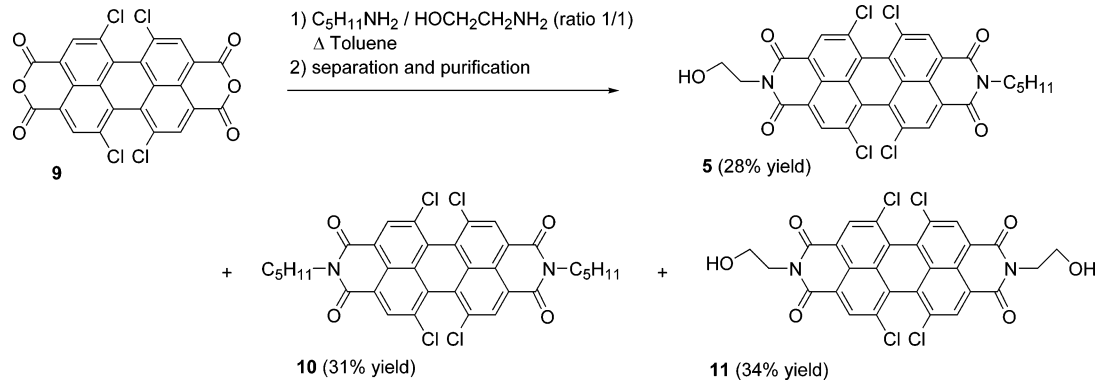

monoacid **4** and PDI monoalcohol **5** in the presence of dicyclohexylcarbodiimide (DCC) as an activating coupling reagent and both 4-(dimethylamino)pyridine (DMAP) and 1-hydroxybenzotriazole (HOBT) afforded dyad **3** in 94% yield (Scheme 2). Using the same reaction, we synthesized TTF **8** as the reference for further studies of dyad **3**.

X-ray Crystallography. Single red crystals were obtained by slow evaporation of a solution containing unsymmetrical PDI **5** in $CHCl_3$ and analyzed by X-ray diffraction. If the packing arrangement of PDI molecules nonsubstituted at the bay region was studied in great details to optimize pigment colors for corresponding applications,[25] this constitutes to our knowledge the unique example described in the literature of the crystallographic structure description for an unsymmetrical PDI derivative (Figure 1).[26]

The crystallographic analysis revealed that the central six-membered ring is highly twisted with two different torsion angles of 35° and 37° associated with bay carbons C2−C1−C15−C16 and C8−C7−C21−C22, respectively (Figure 2). This twist of the carbon framework results from electrostatic repulsion and steric effect among chlorine substituents, and these torsion angles are in good agreement with the value of 36.7° recently reported for a symmetrical tetrachlorosubstituted perylene bis(dicarboximide).[27]

The crystallographic organization of PDI **5** is characterized by a regular stack along the *a* axis, and PDI molecules are all oriented in a head-to-head noncentrosymmetrical manner. Moreover, PDI molecules are shifted one from each other along the main molecular axis, presenting a stair arrangement (Figure 3).

This induces an overlap in which $\pi-\pi$ interactions between two molecules associate the ring *A* of one molecule with the ring *E* of the neighboring PDI in the packing arrangement (Figure 4). It should be noted that this association mode of the network does not correspond to organizations known to date and recently reviewed in the PDI series.[28] The intermolecular distance of 3.49(1) Å between two PDI molecules can be compared to the distance reported between two parallel PDI molecules nonsubstituted at the bay region (between 3.34 and 3.55 Å).[29]

Cyclic Voltammetry. In positive direction, the cyclic voltammogram (Figure 5 and Table 1) of TTF−PDI **3** exhibited two one-electron reversible oxidation waves at

(24) This constitutes an efficient methodology that avoids the preliminary synthesis of 3,4:9,10-perylenetetracarboxylic monoanhydride monoimide derivative: (a) Nagao, Y.; Misono, T. *Bull. Chem. Soc. Jpn*. **1981**, *54*, 1191. (b) Tröster, H. *Dyes Pigm.* **1983**, *4*, 171. (c) Kaiser, H.; Lindner, J.; Langhals, H. *Chem. Ber.* **1991**, *124*, 529. (d) Nagao, Y.; Naito, T.; Abe, Y.; Misono, T. *Dyes Pigm.* **1996**, *32*, 71.

(25) (a) Graser, F.; Hädicke, E. *Liebigs Ann. Chem.* **1980**, 1994. (b) Graser, F.; Hädicke, E. *Liebigs Ann. Chem.* **1984**, 483. (c) Hädicke, E.; Graser, F. *Acta Crystallogr., Sect. C* **1986**, *42*, 189. (d) Hädicke, E.; Graser, F. *Acta Crystallogr., Sect. C* **1986**, *42*, 195. (e) Klebe, G.; Graser, F.; Hädicke, E.; Berndt, J. *Acta Crystallogr., Sect. B* **1989**, *45*, 69. (f) Zugenmaier, P.; Duff, J.; Bluhm, T. L. *Cryst. Res. Technol.* **2000**, *35*, 1095.

(26) According to the Crystallographic Cambridge Data Base.

(27) Chen, Z.; Debije, M. G.; Debaerdemaeker, T.; Osswald, P.; Würthner, F. *ChemPhysChem* **2004**, *5*, 137.

(28) Würthner, F. *Chem. Commun.* **2004**, 1564.

(29) This distance was determined by considering the plane that associates $C_{16}-C_{17}-C_{18}-C_{19}-C_{22}-C_{23}-C_{24}-C_{25}-C_{26}$ carbon atoms of one PDI molecule and the plane involving $C_{02}-C_{03}-C_{04}-C_{05}-C_{08}-C_{09}-C_{10}-C_{11}-C_{12}$ atoms of the neigboring PDI molecule.

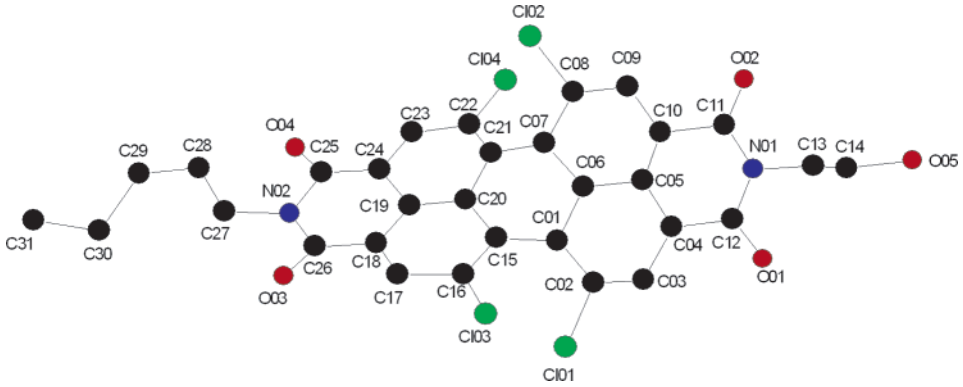

FIGURE 1. View of the crystal structure of unsymmetrical PDI derivative **5** (hydrogen atoms are omitted for clarity).

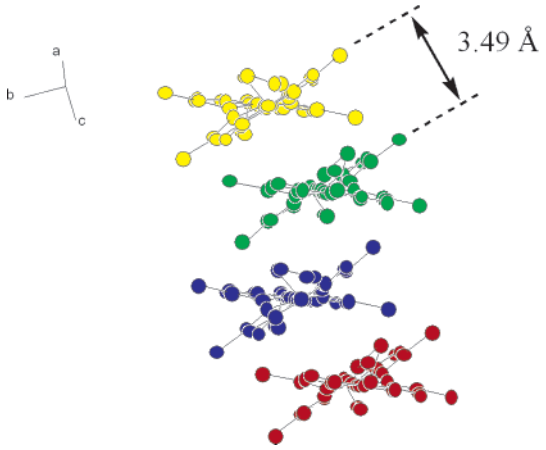

FIGURE 2. Stacking arrangement and intermolecular distance between two PDI units.

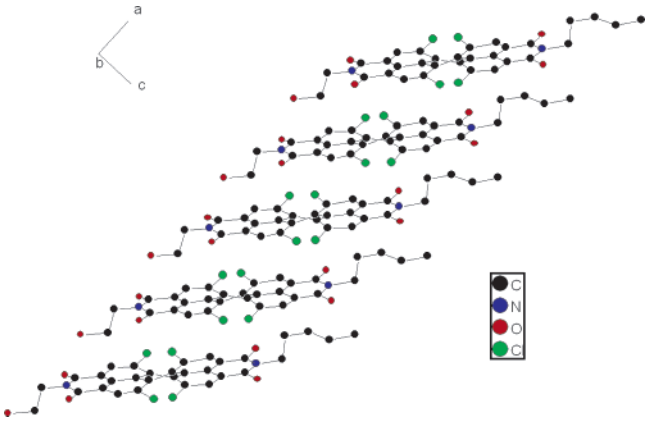

FIGURE 3. Stacking mode arrangement of PDI **5** onto the (*ac*) plane.

$E_{1/2\,ox1}$ = +0.65 V and $E_{1/2\,ox2}$ = +1.05 V (versus AgCl/Ag), corresponding to the successive generation of the cation radical $TTF^{\bullet+}$−PDI and dication TTF^{2+}−PDI. As expected, the oxidation of the PDI moiety was not observed in the potential range of 0.1 M tetrabutylammoniumhexafluorophosphate (TBAHP)/CH_2Cl_2. Indeed, as chlorine atoms at the bay region of the PDI core present electron-withdrawing effects, the oxidation potential of **10** must be shifted to a more positive value by comparison with the oxidation potential (+1.62 V (versus AgCl/Ag)) of the nonsubstituted PDI.[30]

In the negative direction, two one-electron reversible reduction processes were shown for the PDI moiety at $E_{1/2\,red1}$ = −0.32 V and $E_{1/2\,red2}$ = −0.52 V, which were ascribed to the successive formation of the anion radical $TTF-PDI^{\bullet-}$ and dianion $TTF-PDI^{2-}$ (Figure 5). Comparison of different values for dyad **3** with reference compounds **8** and **10** suggests that no significant interaction takes place between both electroactive moieties in the ground state (Table 1).

Electronic Absorption. The UV−visible spectrum of dyad **3** in CH_2Cl_2 shows a wide absorption in the visible range between 400 and 550 nm with an absorption maximum centered at λ = 517 nm (Figure 6, Table 2). This absorption feature could be attributed to the PDI moiety by comparison with UV−visible spectra of references **8** and **10**. Neither significant interaction between TTF and PDI units in the 300−500 nm range nor a new intramolecular charge-transfer band above 600 nm was detected in dyad **3**. The UV−visible absorption spectrum of an equimolar mixture of reference compounds **8** and **10** also exhibits no charge-transfer band and matches the absorption spectrum of dyad **3** on the whole wavelength range.

Steady-State Fluorescence. In comparison with the fluorescence spectrum of PDI **10**, a quantitative quenching (ca. 99.7%) of the PDI fluorescence emission was observed in dyad **3** (Figure 7, Table 2). This phenomenon was ascribed to an intramolecular process as the addition of TTF derivative **8** to a solution of PDI **10** (upon molar ratio of 1:1 between **10** and **8**) induced no change in either shape or intensity in the fluorescence emission of **10**. This weakly fluorescence emission of dyad **3** could be attributed to a photoinduced electron transfer (PET) reaction between PDI and TTF moieties in the dyad for two major reasons: (i) a PET process is thermodynamically favorable as the corresponding free energy (ΔG_{PET}) was estimated to be −1.64 eV (calculated using the Rehm−Weller equation)[31] and (ii) the energy transfer process from ^{1}PDI* to TTF is prohibited according to the energy level of both units (+2.32 and +2.85 eV, respectively)[32] and lack of spectral overlap between the absorption

(30) Lee, S.-K.; Zu, Y.; Herrmann, A.; Geerts, Y.; Müllen, K.; Bard A. J. *J. Am. Chem. Soc.* **1999**, *121*, 3513.

(31) Rehm, D.; Weller, A. *Isr. J. Chem.* **1970**, *8*, 259. For dyad **3**: $\Delta G_{PET} = E$ (ox) − E (red) − E^{0-0} (**10**) − $e^2/4\pi\epsilon r$ with E (ox) = +0.63 eV, E (red) = −0.34 eV, E^{0-0} (**10**) = 2.32 eV, and ϵ = 8.93, r = 6 Å (the distance between the two ions was estimated by geometrical optimization using PM3 semiempirical method).

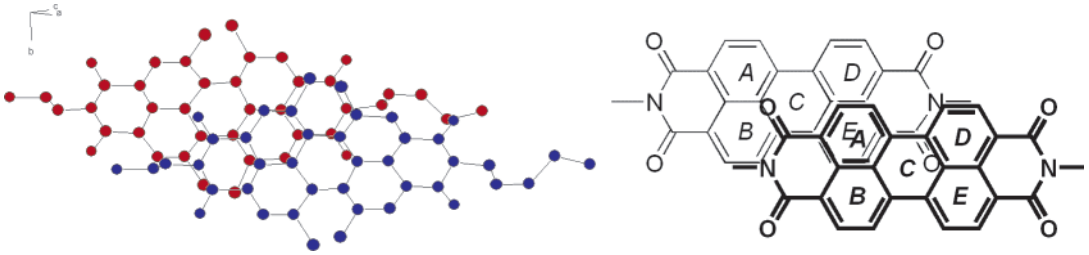

FIGURE 4. $\pi-\pi$ Interactions between two neighboring molecules: crystallographic packing (left) and corresponding scheme (right) in which only PDI cores were considered for clarity.

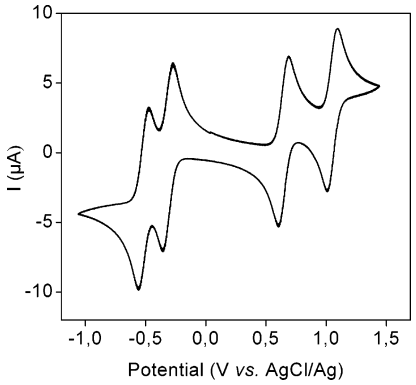

FIGURE 5. Cyclic voltammogram of dyad **3** ($c = 10^{-3}$ M) using nBu$_4$NPF$_6$ 0.1 M in CH_2Cl_2 as supporting electrolyte, AgCl/Ag as the reference, platinum wires as counter and working electrodes, scan rate: 100 mV/s.

TABLE 1. Electrochemical Data for 3 and Reference Compounds[a]

compd	$E_{1/2\ red2}$[b]	$E_{1/2\ red1}$[b]	$E_{1/2\ ox1}$[b]	$E_{1/2\ ox2}$[b]
3	−0.52	−0.32	+0.65	+1.05
8			+0.63	+1.05
10	−0.53	−0.34		

[a] These values (V) were recorded in CH_2Cl_2 solution using nBu$_4$NPF$_6$ ($c = 0.1$ M) as supporting electrolyte, AgCl/Ag as the reference, platinum wires as counter and working electrodes, scan rate: 100 mV/s. [b] V versus AgCl/Ag.

spectrum of TTF unit and the fluorescence spectrum of the PDI unit.

Spectroelectrochemistry and Chemical Oxidation. One of the most interesting properties of TTF results in the possibility to achieve selective oxidation of the TTF unit and to follow the formation of cation radical and dication species by the appearance of new UV−visible absorption bands.[33] Indeed, when one or two electrons are removed from the electron donor TTF, cation radical or dication species thus formed present accepting properties. Consequently, it was expected that the chemical or electrochemical oxidation of TTF (which could be achieved selectively in dyad **3** according to redox potentials of both electroactive units) would hinder the

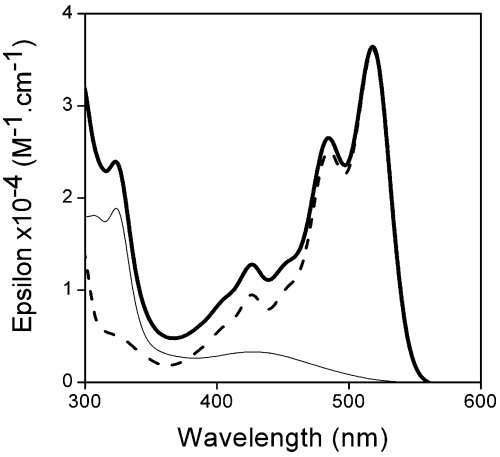

FIGURE 6. Absorption spectra of dyad **3** (bold line) and references TTF **8** (solid line) and PDI **10** (dashed line) in CH_2Cl_2.

TABLE 2. Selected Photophysical Data for Neutral and Oxidized Species of Dyad 3 and References in CH_2Cl_2

	absorption		fluorescence emission	
compound	λ_{max} (nm)[a]	ϵ (M^{-1} cm^{-1})	λ_{max} (nm)	Φ
8	427	3290	–	–
8$^{\bullet+}$	440[b], 760	–	–	–
8^{2+}	654	–	–	–
10	518	56300	544	1
3	517	62640	545	3.4×10^{-3}
3$^{\bullet+}$	440[b], 535, 760	–	545	2.3×10^{-3}
3^{2+}	480[b], 529, 654	–	545	0.16

[a] For oxidized species, data correspond to new absorption band detected by UV−visible spectroelectrochemistry. [b] Broad band centered at the wavelength given.

PET from TTF to PDI units. Therefore, the fluorescence emission of the PDI moiety in dyad **3** should be restored, as it was recently observed in the case of the anthracene−TTF−anthracene triad[17] or TTF−porphyrin dyad.[16] For this purpose, experiments of fluorescence emission measurements coupled to electrochemistry[34] were carried out in CH_2Cl_2 solution at controlled potentials (Figure 8).

The reference fluorescence intensity I_{f0} is taken for the neutral TTF−PDI species at +0.2 V (Figure 8A). In thin layer condition (<100 μm, a conversion time better than 50 s), applying a positive potential step (+0.2 to +0.85 V) led to a fast oxidation of the neutral TTF−PDI species into the cation radical (TTF$^{\bullet+}$−PDI). The formation of the

(32) Values corresponding to the peak of lowest energy featured in absorption spectra or UV−vis spectroelectrochemical spectra recorded in CH_2Cl_2.

(33) (a) Torrance, J. B.; Scott, B. A.; Welber, B.; Kaufman, F. B.; Seiden, P. E. *Phys. Rev. B* **1979**, *19*, 731. (b) Hudhomme, P.; Le Moustarder, S.; Durand, C.; Gallego-Planas, N.; Mercier, N.; Blanchard, P.; Levillain, E.; Allain, M.; Gorgues, A.; Riou, A. *Chem.−Eur. J.* **2001**, *7*, 5070. (c) Khodorkovsky, V.; Shapiro, L.; Krief, P.; Shames, A.; Mabon, G.; Gorgues, A.; Giffard, M. *Chem. Commun.* **2001**, 2736.

(34) Dias, M.; Hudhomme, P.; Levillain, E.; Perrin, L.; Sahin, Y.; Sauvage, F.-X.; Wartelle, C. *Electrochem. Commun.* **2004**, *6*, 325.

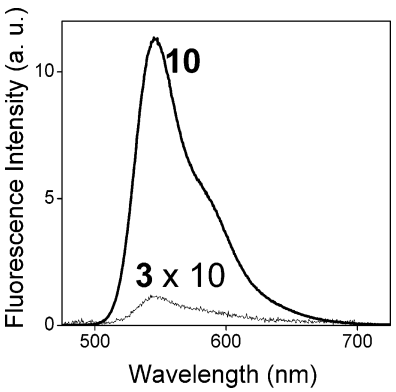

FIGURE 7. Fluorescence spectra of dyad **3** (×10) and compound **10** in CH_2Cl_2 (λ_{exc} = 425 nm; c = ca. 2 × 10^{-6} M).

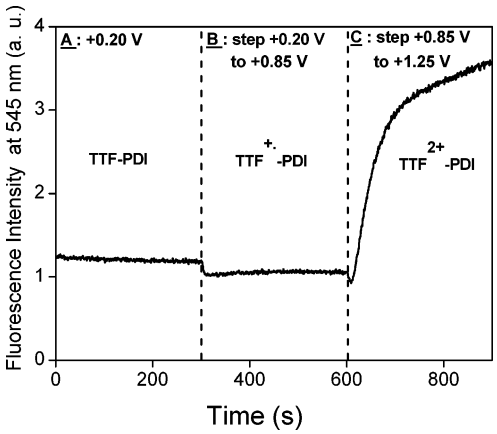

FIGURE 8. Evolution of the fluorescence intensity at 545 nm (λ_{exc} = 490 nm, c = 10^{-3} M in CH_2Cl_2) of dyad **3** at different oxidation states versus time.

cation radical species at this potential was confirmed by UV−visible spectroelectrochemical experiments by a broad absorption in the wavelength range of 350−600 nm and another one centered at 760 nm.[35] During the positive potential step (+0.2 to +0.85 V), the vicinity of the working electrode was irradiated at 490 nm. The fluorescence intensity (I_f), recorded at 545 nm, was displayed in Figure 8B, and surprisingly it was slightly decreased ($I_f < I_{f0}$).

A similar result was already observed with the triad **2** by chemical oxidation. Indeed, a slight decrease of this triad fluorescence intensity was also recorded upon addition of $Fe(ClO_4)$ as oxidative agent and was attributed to an energy transfer.[19] No increase of fluorescence emission was noted in a $TTF^{\bullet+}$−phthalocyanine system, this being attributed to a photoinduced reverse electron-transfer path.[15b] In the same way, an enhanced intermolecular fluorescence quenching of anthracene by $TTF^{\bullet+}$ in comparison with neutral TTF was observed in the case of a polymeric system with pendant anthracene, this intermolecular phenomenon being attributed to a stronger binding between these two π-rich units.[36]

In our case, this behavior could result from both photoinduced energy transfer and reverse photoinduced electron transfer from ^{1}PDI* to $TTF^{\bullet+}$ species. Indeed, energy levels of the first excited state of both moieties were found to be +1.61 eV for $TTF^{\bullet+}$ and +2.32 eV for PDI (Table 2). These values, in line with some spectral overlap between fluorescence emission of PDI and absorption of $TTF^{\bullet+}$ moieties in dyad **3**, agree with energy transfer from ^{1}PDI* to $TTF^{\bullet+}$. On the other hand, the ΔG_{PET} value for oxidative electron transfer process cannot be precisely determined because of the uncertainty concerning the oxidation potential of the PDI unit. Nevertheless, because this latter was superior to +1.95 V and consequently ΔG_{PET} was above −0.97 eV, PET from the PDI moiety to the $TTF^{\bullet+}$ unit could be thermodynamically favorable and thus were not ruled out.

Applying a positive potential step (+0.85 to +1.25 V) led to a fast oxidation of the cation radical ($TTF^{\bullet+}$−PDI) into the dication (TTF^{2+}−PDI). The presence of the dication was also confirmed at +1.25 V by UV−visible spectroelectrochemical experiments by a broad absorption centered at 654 nm.[35] During the positive potential step (+0.85 to +1.25 V), the I_f increases during five minutes but seems to tend toward a stable asymptotical value (Figure 8C). In the same conditions, the reference compound **8** is not fluorescent even when oxidized to $\mathbf{8}^{\bullet+}$ or $\mathbf{8}^{2+}$. This has to be compared to fluorescence studies of neutral and oxidized species of TTF **1** for which **1** and $\mathbf{1}^{\bullet+}$ do not show any luminescence,[37] whereas $\mathbf{1}^{2+}$ was found to display a fluorescence band.[38,39] This difference probably results from the substitution pattern of **8** in comparison with pristine TTF **1**. Consequently, the fluorescence intensity enhancement is not due to TTF^{2+} emission in dyad **3**.

Energy transfer from PDI to TTF^{2+} in $\mathbf{3}^{2+}$ could exist as the energy position of the lowest singlet excited state of TTF^{2+} unit was estimated at +1.90 eV. TTF dicationic species behave as electron acceptors,[39] and a reverse electron transfer from PDI to TTF^{2+} units should not be ruled out as a potential relaxation path of ^{1}PDI* (the value of the corresponding ΔG_{PET} could not be calculated accurately for the same reasons as before). Such kinetic processes should be less efficient than the ones involved in the case of $\mathbf{3}^{\bullet+}$ because the fluorescence emission of the PDI unit is slowly partially restored.

Chemical oxidation experiments were also performed to confirm the behavior of this TTF^{2+}−PDI species. Thus, dyad **3** in CH_2Cl_2 solution was treated by an excess of (diacetoxyiodo)benzene in the presence of triflic acid ($PhI(OAc)_2/CF_3SO_3H$) used as an oxidizing reagent.[40] The fluorescence emission was then recorded every 3 min without any supplementary addition of oxidizing agent. The fluorescence intensity reached a limit value, $I_{f\infty}$, after about 70 min. This value corresponds to around 16% of the fluorescence intensity of PDI **10** recorded with the same experimental conditions (Figure 9).

Consequently, the fluorescence emission is partially recovered at the TTF^{2+}−PDI stage, while in the case of

(35) Spanggaard, H.; Prehn, J.; Nielsen, M. B.; Levillain, E.; Allain, M.; Becher, J. *J. Am. Chem. Soc*. **2000**, *122*, 9486.
(36) De Cremiers, H. A.; Clavier, G.; Ilhan, F.; Cooke, G.; Rotello, V. M. *Chem. Commun*. **2001**, 2232.
(37) Zimmer, K.; Gödicke, B.; Hoppmeier, M.; Meyer, H.; Schweig, A. *Chem. Phys.* **1999**, *248*, 263.
(38) Bryce, M. R. *J. Mater. Chem.* **2000**, *10*, 589.
(39) (a) Ashton, P. R.; Balzani, V.; Becher, J.; Credi, A.; Fyfe, M. C. T.; Mattersteig, G.; Menzer, S.; Nielsen, M. B.; Raymo, F. M.; Stoddart, J. F.; Venturi, M.; Williams, D. J. *J. Am. Chem. Soc.* **1999**, *121*, 3951.
(40) Giffard, M.; Mabon, G.; Leclair, E.; Mercier, N.; Allain, M.; Gorgues, A.; Molinié, P.; Neilands, O.; Krief, P.; Khodorkovsky V. *J. Am. Chem. Soc.* **2001**, *123*, 3852.

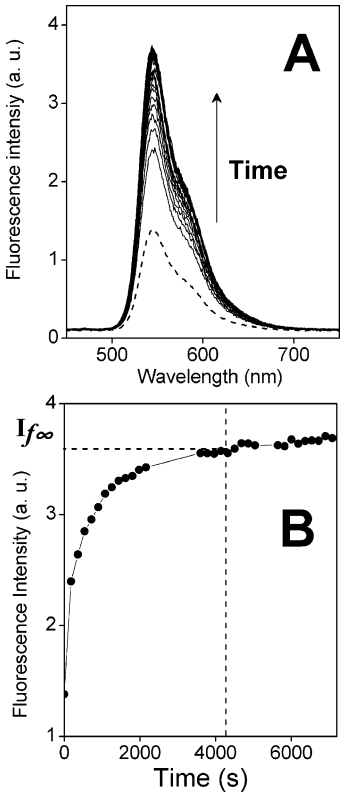

FIGURE 9. (A) Fluorescence emission spectra of dyad **3** recorded before (– – –) and after addition of an excess of (diacetoxyiodo)benzene in the presence of triflic acid $(PhI(OAc)_2/CF_3SO_3H$ (spectra were recorded every 3 min). (B) Evolution of the fluorescence intensity of dyad **3** versus time monitored at 545 nm ($c = 2 \times 10^{-6}$ M in CH_2Cl_2, $\lambda_{exc} = 425$ nm).

the TTF–porphyrine dyad[16] and anthracene–TTF–anthracene triad[17] the fluorescence normally reappeared with the formation of the $TTF^{\bullet+}$–acceptor species. On the other hand, to our knowledge, in all $TTF^{\bullet+}$–fluorophore systems where no increase of fluorescence emission was noted ($TTF^{\bullet+}$–phthalocyanine dyad[15b] and $TTF^{\bullet+}$–PDI–TTF triads[19]), no further oxidation to TTF^{2+} species was carried out.

To study the reversibility of the process in dyad **3**, zinc powder was then added in excess to this solution to reduce TTF^{2+}–PDI into TTF^{0}–PDI species. The initial fluorescence spectrum of dyad **3** was completely recovered (Figure 10).

Applying a negative potential step (+0.2 to −0.90 V) led to a fast reduction of the neutral TTF–PDI species into the dianion ($TTF–PDI^{2-}$), and as expected, the total quenching of fluorescence of dyad **3** coincides with the first reduction peak of the PDI moiety (Figure 11).[34]

Consequently, the fluorescence intensity of the solution of dyad **3** can be reversibly modulated by the sequential chemical or electrochemical oxidation and reduction processes.

Conclusion

In conclusion, the synthesis and spectroscopic studies of the first described TTF–PDI dyad are presented. Depending on the oxidation state of the TTF, the emission fluorescence intensity of this dyad in solution can

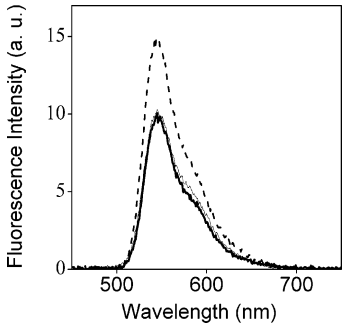

FIGURE 10. Fluorescence emission spectra of dyad **3** (bold line), of dyad **3** after oxidation to TTF^{2+}–PDI (dashed line), and of dyad **3** after oxidation and reduction paths (solid line) ($c = 1.5 \times 10^{-6}$ M in CH_2Cl_2, $\lambda_{exc} = 425$ nm).

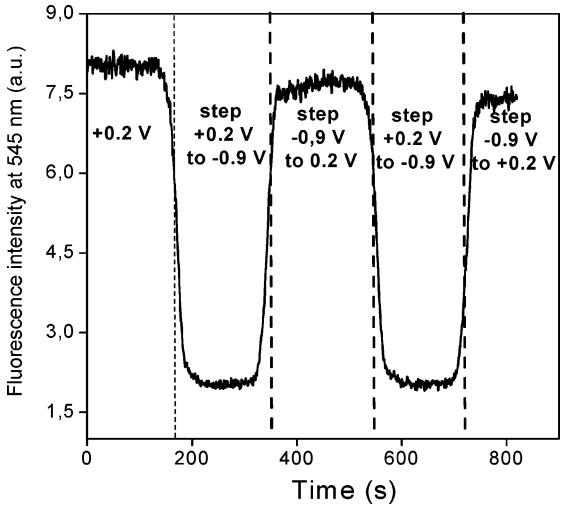

FIGURE 11. Evolution of the fluorescence intensity at 545 nm ($\lambda_{exc} = 490$ nm, $c = 10^{-3}$ M in CH_2Cl_2) of dyad **3** when PDI was reduced versus time.

be reversibly modulated by either electron or energy transfer. Such unique behavior can be attributed to the peculiar properties of the redox-active TTF linked to the PDI acceptor which fluoresces intrinsically. This dyad **3** could therefore be considered as a new kind of redox molecular switch with delayed optical response.

Experimental Section

Synthesis. 2-Ethyloxycarbonyl-6,7-bis(methylsulfanyl)-TTF 8. To a suspension of TTF monocarboxylic acid **4**[23] (102 mg, 0.3 mmol) in anhydrous CH_2Cl_2 (20 mL) were added successively under nitrogen atmosphere HOBT (41 mg, 0.3 mmol), DCC (68 mg, 0.33 mmol), DMAP (37 mg, 0.3 mmol), and then anhydrous ethanol (35 μL, 0.6 mmol). The reaction mixture was stirred at room temperature during 2 days until a clear orange solution was obtained. After concentration under reduced pressure, the residue was purified by column chromatography on silica gel (petroleum ether/CH_2Cl_2, 30/70 as the mixture of solvents) and compound **8** was isolated as red crystals (105 mg, 95% yield); mp 102 °C (CH_2Cl_2/petroleum ether); ^{1}H NMR (500 MHz, $CDCl_3$): 7.33 (s, 1H), 4.26 (q, J = 7 Hz, 2H), 2.42 and 2.41 (2s, 6H), 1.32 (t, J = 7 Hz, 3H); ^{13}C NMR (125 MHz, $CDCl_3$): 159.3, 131.5, 128.5, 128.0, 127.1, 113.2, 109.2, 62.0, 19.2, 19.2, 14.2; MS (MALDI-TOF, dithranol): 368 ($M^{+\bullet}$). Elemental analysis for $C_{11}H_{12}O_2S_6$ (368.60): calcd C, 35.84; H, 3.28. Found C, 35.59; H, 3.37.

***N*-2′-Hydroxyethyl-*N*′-pentyl-1,6,7,12-tetrachloroperylene-3,4:9,10-bis(dicarboximide) 5.** To a solution of 1,6,7,12-tetrachloroperylene 3,4:9,10-tetracarboxylic dianhydride **9** (10 g; 18.9 mmol) in toluene (10 mL) were added simultaneously *n*-pentylamine (2.2 mL, 18.9 mmol) and ethanolamine (1.2 mL, 18.9 mmol). The reaction mixture was heated under reflux for 24 h. The solvent was removed under reduced pressure, and symmetrical *N*,*N*′-2′,2″-dihydroxyethyl-1,6,7,12-tetrachloroperylene-3,4:9,10-tetracarboxylic diimide **11** (4 g, 34% yield) was precipitated after addition of CH_2Cl_2 (200 mL). The filtrate was concentrated under reduced pressure and purified by column chromatography on silica gel. Symmetrical derivative **10** was first isolated using CH_2Cl_2 as the eluent (3.1 g, 31% yield), and then unsymmetrical compound **5** was obtained using CH_2Cl_2/EtOAc (1/4) as the mixture of eluents (3.4 g, 28% yield). ^{1}H NMR ($CDCl_3$, 500 MHz): δ 8.62 (s, 2H), 8.60 (s, 2H), 4.50 (t, J = 7.5 Hz, 2H), 4.30−4.10 (br s, 1H), 4.20 (t, J = 7.5 Hz, 2H), 4.00 (t, J = 7 Hz, 2H), 1.80 (m, 2H), 1.50 (m, 4H), 0.95 (t, J = 7.5 Hz, 3H); IR (KBr, cm^{-1}): ν 3436 (broad, OH), 1702, 1658, 1587; MS (MALDI-TOF, dithranol): 642 (M + 2H)$^+$.

***N*,*N*′-Dipentyl-1,6,7,12-tetrachloroperylene-3,4:9,10-bis(dicarboximide) 10.** ^{1}H NMR ($CDCl_3$, 500 MHz): 8.67 (s, 4H), 4.20 (t, J = 7.5 Hz, 4H), 1.75 (t, J = 7.3 Hz, 4H), 1.41 (m, 8H), 0.93 (t, J = 7 Hz, 6H); ^{13}C NMR ($CDCl_3$, 125 MHz): 162.2, 135.3, 132.9, 131.4, 128.6, 123.2, 40.9, 29.1, 27.7, 22.4, 14.0; IR (KBr, cm^{-1}): ν 1703, 1665, 1588; MS (DCI$^+$): 668 (M + 2H)$^+$. Elemental analysis for $C_{34}H_{26}Cl_4O_2S_4$ (668.39): calcd C, 61.10; H, 3.92; N, 4.19. Found C, 59.89; H, 3.73; N, 4.24.

***N*,*N*′-Bis(2′-hydroxyethyl)-1,6,7,12-tetrachloroperylene-3,4:9,10-bis(dicarboximide) 11.** ^{1}H NMR (DMSO-d_6, 500 MHz): δ 8.75 (s, 4H), 4.35 (br t, 4H), 4.20 (br t, 4H), 3.40−3.20 (br m, 2H); IR (KBr, cm^{-1}): ν 3424 (broad, OH), 1703, 1663, 1588; MS (MALDI-TOF, dithranol): 616 (M + 2H)$^+$.

Dyad 3. To a suspension of TTF monocarboxylic acid **4** (170 mg, 0.5 mmol) in anhydrous CH_2Cl_2 (30 mL) were added successively under nitrogen atmosphere HOBT (68 mg, 0.5 mmol), DCC (113 mg, 0.55 mmol), DMAP (61 mg, 0.5 mmol), and then monoalcohol derivative **5** (321 mg, 0.5 mmol). The reaction mixture was stirred at room temperature during 5 days. After concentration under reduced pressure, the residue was purified by column chromatography on silica gel [CH_2Cl_2 and then CH_2Cl_2/EtOAc (95/5)] and dyad **3** was isolated as orange crystals (290 mg, 94% yield); mp 207 °C (CH_2Cl_2/petroleum ether); ^{1}H NMR (500 MHz, $CDCl_3$): 8.68 and 8.70 (2 s, 4H), 7.30 (s, 1H), 4.60 (m, 4H), 4.20 (t, 2H), 2.37 and 2.40 (2s, 6H), 1.80 (m, 2H), 1.40 (m, 4H), 0.95 (t, 3H); ^{13}C NMR (125 MHz, $CDCl_3$): 162.3, 162.2, 159.0, 135.4, 135.3, 133.1, 133.0, 132.9, 132.8, 132.5, 131.4, 131.3, 128.9, 128.4, 127.8, 127.6, 127.5, 123.3, 123.2, 122.7, 112.7, 109.4, 63.0, 40.9, 39.3, 29.1, 27.7, 22.4, 19.2, 13.9; MS (MALDI-TOF): 964 (M$^{+\bullet}$). Elemental analysis for $C_{40}H_{26}Cl_4N_2O_6S_6$ (964.85): calcd C, 49.79; H, 2.72; N, 2.90; found C, 48.96; H, 2.63; N, 2.76.

X-ray Crystallographic Analysis. X-ray single-crystal diffraction data were collected at 293 K on a STOE-IPDS diffractometer equipped with a graphite monochromator utilizing Mo Kα radiation (λ = 0.71073 Å). The structure was solved by direct methods using SIR92[41] and refined on F^2 by full matrix least-squares techniques using SHELXL-97[42] with anisotropic thermal parameters for Cl atoms and isotropic ones for C, N, and O atoms. Absorption was corrected by a multiscan technique, and H atoms were included in the calculation without refinement.

Crystallographic data of compound **5**: Single red crystals (0.50 × 0.08 × 0.05 mm^3) were grown at 293 K by slow evaporation of a $CHCl_3$ solution containing **5**. $C_{31}H_{20}Cl_4N_2O_5$, M = 642.29 g·mol^{-1}; monoclinic, space group Ia, a = 12.859 (1) Å, b = 14.567(2) Å, c = 14.729(2) Å, β = 92.67 (1)°, V = 2756.0(6) Å^3, Z = 4, ρ_{calcd} = 1.548 g·cm^{-3}, λ(Mo Kα) = 0.71073 Å, 13 021 reflections (1.97 < θ < 25.77°) were collected at 293 K, 4902 unique reflections and 1526 reflections with $I > 2\sigma(I)$ used in refinement, 189 parameters, R1 = 0.0578, wR2 = 0.1245, GOF = 0.764.

Steady-State Spectroscopy. All solvents used were spectroscopic grade and were used as commercially available. Electronic absorption spectra were recorded with a spectrometer from a commercial supplier. Fluorescence spectra were recorded in nondeoxygenated solvents at 20 °C with a fluorimeter equipped with rapid monochannel detection and continuous excitation source. We did not find any difference in emission properties with and without degassing the solutions. Quantum yields were determined using cresyl violet as a standard reference (Φ_f = 0.54 at 20 °C in MeOH).[43]

Electrochemistry and Spectroelectrochemistry. Cyclic voltammetry was performed in a three-electrode cell equipped with a platinum millielectrode and a platinum wire counterelectrode. A silver wire served as a quasi-reference electrode, and its potential was checked against the ferricinium/ferrocene couple (Fc^+/Fc) before and after each experiment. The electrolytic media involved CH_2Cl_2 and 0.2 M of TBAHP. All experiments were performed in a glovebox containing dry, oxygen-free (<1 ppm) argon, at room temperature. Electrochemical experiments were carried out with an EGG PAR 273A potentiostat with positive feedback compensation. On the basis of repetitive measurements, absolute errors on potentials were found to be around ±5 mV.

The setup of UV−visible and fluorescence spectroelectrochemical experiments was already described in refs 34 and 44. The conversion time of the cell was less than 1 s at 20 μm and less than 100 s at 200 μm.

Acknowledgment. This work was supported by grants from the Région Pays de la Loire-CNRS-TotalFinaElf (for L.P.) and the Conseil Général du Maine et Loire (for J.B.). We acknowledge ADEME and CEA through the Cellules Solaires Photovoltaïques Plastiques (CSPVP) research program. We thank BASF-AG, Ludwigshafen, for providing 1,6,7,12-tetrachloroperylenetetracarboxylic dianhydride **9**.

Supporting Information Available: ^{1}H and ^{13}C NMR spectra of dyad **3** and references **8** and **10**. Crystallographic data, tables of bond distances and angles, positional parameters, general displacement parameters, and supplementary views of the crystallographic structure of compound **5**. This material is available free of charge via the Internet at http://pubs.acs.org.

JO050766N

(41) *SIR92*, a program for crystal structure solution. Altomare, A.; Cascarano, G.; Giacovazzo, C.; Guagliardi, A. *J. Appl. Crystallogr.* **1993**, *26*, 343.

(42) Sheldrick, G. M. *SHELX97*, which includes *SHELXS97*, *SHELXL97*, *CIFTAB* (and *SHELXA*), programs for crystal structure analysis (release 97-2); University of Göttingen: Göttingen, Germany, 1998.

(43) Magde, D.; Brannon, J. H.; Cremers, T. L.; Olmsted, J. *J. Phys. Chem.* **1979**, *83*, 696.

(44) Gaillard, F.; Levillain, E. *J. Electroanal. Chem.* **1995**, *398*, 77.